Probing the nuclear energy functional at band termination

Honorata Zduńczuk,[1,*] Wojciech Satuła,[1,2,†] and Ramon A. Wyss[2,‡]
[1]*Institute of Theoretical Physics, University of Warsaw, ul. Hoża 69, PL-00 681 Warsaw, Poland*
[2]*KTH (Royal Institute of Technology), AlbaNova University Center, SE-106 91 Stockholm, Sweden*
(Received 29 June 2004; revised manuscript received 22 November 2004; published 9 February 2005)

A systematic study of terminating states in the $A \sim 50$ mass region using the self-consistent Skyrme-Hartree-Fock model is presented. The objective of this study is to demonstrate that the terminating states, due to their intrinsic simplicity, offer unique and so far unexplored opportunities to study different aspects of the effective *NN* interaction or nuclear local energy density functional. In particular, we show that the agreement of the calculations to the data depends on the spin fields and the spin-orbit term which, in turn, allows us to constrain the appropriate Landau parameters and the strength of the spin-orbit potential. The present study reveals that the structure and energy of terminating states can be used as a tool to differentiate among the many Skyrme force parametrizations.

DOI: 10.1103/PhysRevC.71.024305 PACS number(s): 21.30.Fe, 21.60.Jz

I. INTRODUCTION

Modern mean-field calculations describing nuclear structure physics are increasingly based on effective forces like Skyrme or Gogny or on an effective Lagrangian such as the relativistic mean field (RMF). A shortcoming of this approach, however, is the existence of a large number of different realizations of the force parameters, in particular for Skyrme and RMF. In other words, although effective forces or Lagrangians successfully account for the variety of low energy nuclear structure excitations, there is no consensus with respect to the different parameter sets of the forces. The problem relates to the fact that effective force parameters are adjusted to certain experimental observables that are not uniquely defined. Hence, depending on the choice of force parameters, predictions of effective forces differ greatly, particularly when one departs from the line of stability. The challenge today is to find those relevant observables that can be used to unify the different parameter sets and at the same time provide reliable predictions for unstable nuclei.

In this paper we propose a novel method to utilize high-spin data to constrain specific force parameters. Our investigation focuses on Skyrme forces but our approach can be applied to RMF, Gogny, and other forces. The method is based on a direct comparison of the excitation energies of terminating states (which are maximum-spin states within a given *sp* configuration) for two carefully selected configurations. By limiting ourselves to the study of band terminating states only, we access the regime of essentially unperturbed *sp* motion, where correlations going beyond the mean field are expected to be strongly suppressed. Indeed, the success of simple Nilsson-Strutinsky calculations of terminating bands by Ragnarsson and coworkers (for a review see [1]) nicely confirms the structural purity and *sp* nature of the terminating states. The present study reveals that the excitation energy of the selected terminating states probes in particular two aspects of effective forces: (i) the strength of the spin fields and (ii) the spin-orbit (ℓs) potential.

The spin fields originate from the time-odd components of the Skyrme-Hartree-Fock (SHF) method, of which there is limited knowledge. Direct studies of these terms are not only scarce but also in many cases inconclusive; see [2] and references quoted therein. In contrast, we show that the excitation energy of the terminating states allows the direct study of these terms. Indeed, our results clearly indicate that the terminating states can be used to unify the coupling strength parameters of the spin fields.

Within the mean-field approach, the ℓs splitting is usually studied via the comparison of theoretical and experimental single-particle (*sp*) energies of the ℓs doublet. The requirement is that both ℓs partners should be simultaneously occupied [3,4]. The method assumes that under such conditions the core polarization effects, which are known to modify strongly *sp* energies [5,6], are similar for ℓs partners and therefore do not affect the ℓs splittings, at least not in a major way.

This approach requires by definition precise empirical knowledge of the *sp* energies of deep-hole states, which are difficult to measure. In addition, particle vibration coupling may contribute to the splitting and perturb the pure *sp* picture. Unfortunately, the available data on ℓs splittings and their isotopic or isotonic dependence are both scarce and uncertain. For example, in the $A \sim 40$ mass region, which is of primary interest in this work, the most recent evaluations [7] give $\Delta\varepsilon_{d_{3/2}-d_{5/2}} \approx 6$ MeV in ^{40}Ca and $\approx$5 MeV in ^{48}Ca, while older works give $\Delta\varepsilon_{d_{3/2}-d_{5/2}} \approx 6.8$ MeV [8], $\approx$7.3 MeV [9], and $\approx$7.7 MeV [10] in ^{40}Ca and $\approx$5.3 MeV [10] in ^{48}Ca. More detailed information on *sp* levels can be found in Ref. [11].

The new method proposed here to determine the coupling strength of the time-odd spin fields and ℓs term has clear advantages over the standard method mentioned at the beginning: (i) it uses terminating states that are probably the best examples of unperturbed single-particle motion; (ii) the terminating states are uniquely defined, implying that configuration mixing going beyond mean field is expected to

*Electronic address: zdunczuk@fuw.edu.pl.
†Electronic address: satula@fuw.edu.pl.
‡Electronic address: wyss@kth.se.

be marginal; (iii) shape polarization is included automatically within the calculations scheme and no further *ad hoc* assumptions are necessary; (iv) only observables are calculated and the effective-mass-dependent *sp* SHF energies are not used at any time, and (v) a wide set of rather precise experimental data is already available throughout the periodic table.

The paper is organized as follows. Section II shows the relation between the ℓs potential and the energy difference of the selected terminating states. An overview of the available empirical data is presented. Section III briefly recalls the local energy density functional (LEDF) formulation of the SHF method. Section IV reveals the problems inherent to the spin fields from the Skyrme-force-induced local energy density functional (S-LEDF) in $N \sim Z$ nuclei both in the ground state and at band termination. It is shown that a unification of spin fields cures these problems and leads to a unified description of terminating states. The remaining discrepancy between experiment and theory can further be reduced by tuning (weakening) the strength of the spin-orbit interaction as shown in Sec. V. Our results also show that some of the Skyrme forces are outside the range of acceptable deviations to the data and should be dismissed in nuclear structure calculations. All SHF calculations presented in this paper were done using the SHF code HFODD of Dobaczewski, Dudek, and Olbratowski [12,13].

II. EXPERIMENTAL DATA

In this study we select the $d_{3/2}^{-1} f_{7/2}^{n+1}$ and $f_{7/2}^{n}$ configurations in $A \sim 50$, $20 \leqslant Z < N \leqslant 24$ nuclei, where n denotes the number of valence particles outside the ^{40}Ca core. The difference ΔE between the excitation energies of states terminating within the $d_{3/2}^{-1} f_{7/2}^{n+1}$ and $f_{7/2}^{n}$ configurations is dominated by the size of the magic gap 20. The magnitude of the magic gap 20 is in turn directly related to the strength of the ℓs-potential. Indeed, for the spherical Nilsson Hamiltonian [14], i.e., the three-dimensional harmonic-oscillator (HO) potential augmented by a one-body spin-orbit $-2\kappa\hbar\omega_o \boldsymbol{\ell s}$ and orbit-orbit $-\kappa\mu\hbar\omega_o \boldsymbol{\ell}^2$ term, one has

$$\hat{H}_{\text{Nilsson}} - \tfrac{3}{2}\hbar\omega_o = \hbar\omega_o\{N - \kappa[2\boldsymbol{\ell s} + \mu(\boldsymbol{\ell}^2 - \langle \boldsymbol{\ell}^2 \rangle_N)]\}. \tag{1}$$

Hence, within the Nilsson model, which is considered to be a fundamental approximation for the nuclear mean-field potential, one obtains from Eq. (1) the magnitude of the magic gap 20, or more precisely the $f_{7/2} - d_{3/2}$ splitting:

$$\Delta e_{20} = \hbar\omega_o(1 - 6\kappa - 2\kappa\mu). \tag{2}$$

This equation indicates that the magnitude of the magic gap 20 depends on three major factors: the bulk properties of the potential characterized by $\hbar\omega_o$, the flat-bottom and surface properties entering through the orbit-orbit term $\sim\mu$, and the strength of the spin-orbit term κ. In principle, all three terms influence the magic gap 20. However, there exists a clear hierarchy with respect to these effects. In light nuclei, the nuclear potential resembles the pure HO, thus $\mu \sim 0$; i.e., the flat-bottom and the surface-related effects are much less influential than the spin-orbit term. On the other hand, $\hbar\omega_o$ determines the global energy scale in low energy nuclear physics. This energy scale, as well as other bulk properties of potential interest in the context of the present discussion such as mean-square radius, is rather well constrained by the data not only within the Nilsson-Strutinsky model, but also within the self-consistent approaches. Hence, even small variations of the $\hbar\omega_o$ related terms for light nuclei will ultimately destroy any agreement for heavy nuclei and impair in general the good agreement between theory and experiment. Although Eq. (2) pertains to the $f_{7/2} - d_{3/2}$ splitting, the conclusion drawn above can safely be extended to heavier nuclei since there $\mu \to 1/2$ as a consequence of the approximate pseudo-SU(3) symmetry [15–17].

All available experimental data on the terminating states for $f_{7/2}^{n}$ and $d_{3/2}^{-1} f_{7/2}^{n+1}$ configurations in $A \sim 50$, $20 \leqslant Z < N \leqslant 24$ nuclei where both states are known are listed in Table I. In the present data set we have excluded $N = Z$ nuclei since in those nuclei the terminating state $d_{3/2}^{-1} f_{7/2}^{n+1}$ is not uniquely defined. The differences in excitation energies ΔE_{exp} listed in the last column of Table I are fairly constant. The mean value $\overline{\Delta E_{\text{exp}}} = 5.489$ MeV while the standard deviation $\sigma = 0.251$ MeV, i.e., at the level of $\sim$5% only. This suggests that the bulk part of ΔE_{exp} is indeed related to the energy of $1p$-$1h$ excitation across the gap 20 and that polarization effects are either weak or, most likely, canceled out.

III. SKYRME-HARTREE-FOCK LOCAL ENERGY DENSITY FUNCTIONAL

The starting point of the SHF approach is an energy density functional which, in the isoscalar-isovector $t = 0, 1$ representation, takes the form

$$\mathcal{E}^{\text{Skyrme}} = \sum_{t=0,1} \int d^3\boldsymbol{r}\big[\mathcal{H}_t^{(\text{TE})}(\boldsymbol{r}) + \mathcal{H}_t^{(\text{TO})}(\boldsymbol{r})\big]. \tag{3}$$

The local energy density functional $\mathcal{H}$ (LEDF) is uniquely expressed as a bilinear form of time-even (TE) $\rho, \tau, \overleftrightarrow{J}$ and time-odd (TO) $\boldsymbol{s}, \boldsymbol{T}, \boldsymbol{j}$ local densities and currents, and by their derivatives

$$\begin{aligned}\mathcal{H}_t^{(\text{TE})}(\boldsymbol{r}) = {} & C_t^{\rho}\rho_t^2 + C_t^{\Delta\rho}\rho_t\Delta\rho_t + C_t^{\tau}\rho_t\tau_t \\ & + C_t^{J}\overleftrightarrow{J}_t^{\,2} + C_t^{\nabla J}\rho_t\nabla\cdot\boldsymbol{J}_t,\end{aligned} \tag{4}$$

$$\begin{aligned}\mathcal{H}_t^{(\text{TO})}(\boldsymbol{r}) = {} & C_t^{s}\boldsymbol{s}_t^2 + C_t^{\Delta s}\boldsymbol{s}_t\Delta\boldsymbol{s}_t + C_t^{T}\boldsymbol{s}_t\cdot\boldsymbol{T}_t + C_t^{j}\boldsymbol{j}_t^2 \\ & + C_t^{\nabla j}\boldsymbol{s}_t\cdot(\nabla\times\boldsymbol{j}_t).\end{aligned} \tag{5}$$

The division of the LEDF into TE and TO parts is very convenient since the latter contributes only when time reversal symmetry is broken.

In the above formulas $\overleftrightarrow{J}_t^{\,2} \equiv \sum_{\mu\nu} J_{\mu\nu,t}^2$ while the vector spin-orbit density $\boldsymbol{J}_t$ is not an independent quantity but constitutes an antisymmetric part of the tensor density; i.e., $\boldsymbol{J}_t \equiv \sum_{\mu\nu}\epsilon_{\mu\nu}J_{\mu\nu,t}$. Definitions of all local densities and currents $\rho, \tau, \overleftrightarrow{J}, \boldsymbol{s}, \boldsymbol{T}, \boldsymbol{j}$ can be found in numerous references and will not be repeated here. We follow the notation used in Refs. [12,23,24] where references to earlier works can be found as well.

TABLE I. Spins and excitation energies of terminating states in $20 \leqslant Z < N \leqslant 24$ nuclei. The first two columns are representative of the $f_{7/2}^n$ configuration where n denotes the number of valence particles outside the ^{40}Ca core. The next two columns are representative of the $d_{3/2}^{-1} f_{7/2}^{n+1}$ configuration involving the $1p$-$1h$ proton excitation across the magic gap 20. The relative excitation energies between the two configurations are given in the last column.

Ref.	$f_{7/2}^n$		$d_{3/2}^{-1} f_{7/2}^{n+1}$		$\Delta E_{\rm exp}$
	$E[I_{\rm max}]$	$I_{\rm max}$	$E[I_{\rm max}]$	$I_{\rm max}$	
$^{42}_{20}$Ca$_{22}$ [18]	3.189	6^+	8.297	11^-	5.108
$^{44}_{20}$Ca$_{24}$ [19]	10.568	8^+	5.088	13^-	5.480
$^{44}_{21}$Sc$_{23}$ [20]	9.141	11^+	3.567	15^-	5.574
$^{45}_{21}$Sc$_{24}$ [21]	5.417	$23/2^-$	11.022	$31/2^+$	5.605
$^{45}_{22}$Ti$_{23}$ [19]	7.143	$27/2^-$	13.028	$33/2^+$	5.885
$^{46}_{22}$Ti$_{24}$ [19]	10.034	14^+	15.549	17^-	5.515
$^{47}_{23}$V$_{24}$ [22]	10.004	$31/2^-$	15.259	$35/2^+$	5.255

By taking an expectation value of the Skyrme force over the Slater determinant, one obtains the LEDF (3)–(5) with 20 coupling constants C that are expressed uniquely through the 10 parameters x_i, t_i, $i = 0, 1, 2, 3$, and W, α of the standard Skyrme force. The appropriate formulas can be found, e.g., in Refs. [23,24]. Because of the local gauge invariance (which includes the Galilean invariance) of the Skyrme force [23,25], only 14 coupling constants C are independent quantities. The local gauge invariance links three pairs of time-even and time-odd constants in the following way:

$$C_t^j = -C_t^\tau, \qquad C_t^J = -C_t^T, \qquad C_t^{\nabla j} = C_t^{\nabla J}. \tag{6}$$

Because the SHF approach uses interaction-induced coupling constants C, it constitutes a restricted version of the local energy density theory of the Hohenberg-Kohn-Sham [26–28] type. However, only very few SHF approaches rigidly enforce the Skyrme-force-related values of C, which comprise SkP [29], SkXc [30], and SLy5 [31]. Other forces studied here, including SLy4 [31], SIII [32], SkO [33], and SkM* [34] disregard the tensor terms by setting $C_t^J = C_t^T \equiv 0$. This is done not only for practical reasons (these terms are the most difficult technically) but also because of the lack of clear experimental information that would allow us to make reasonable estimates of their strengths. Moreover, in the case of SkO we were forced to set $C_t^{\Delta s} \equiv 0$ to ensure convergence. All versions of the LEDF that use the Skyrme-force-induced C values, including those taking $C_t^J = C_t^T \equiv 0$, will be called the Skyrme-LEDF (S-LEDF).

IV. THE SPIN FIELDS

The values of the coupling constants of the spin fields, $C_t^s \boldsymbol{s}^2$ and $C_t^{\Delta s} \boldsymbol{s} \cdot \Delta \boldsymbol{s}$, emerging from the Skyrme force appear to be more or less accidental. This is illustrated in Fig. 1, which shows the isoscalar Landau parameters g_0 and g_1 calculated for the Skyrme forces under study. The Landau parameters are related to the LEDF strengths in the following way [24]:

$$g_0 = N_0\big(2C_0^s + 2C_0^T \beta \rho_0^{2/3}\big), \qquad g_1 = -2N_0 C_0^T \beta \rho_0^{2/3}, \tag{7}$$

$$g_0' = N_0\big(2C_1^s + 2C_1^T \beta \rho_0^{2/3}\big), \qquad g_1' = -2N_0 C_1^T \beta \rho_0^{2/3}, \tag{8}$$

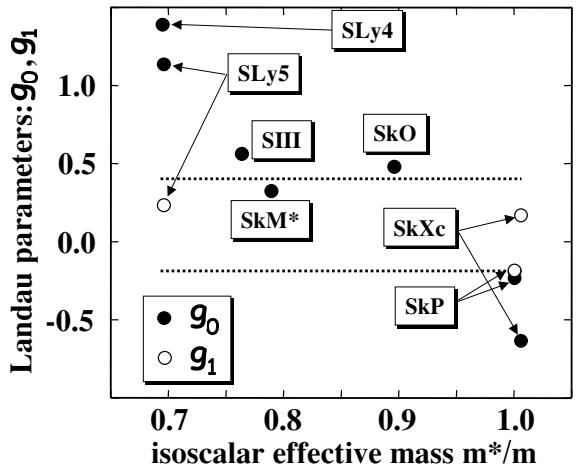

FIG. 1. Isoscalar Landau parameters g_0 (solid circles) and g_1 (open circles) for various Skyrme forces. Vertical lines mark the values $g_0 = 0.4$ and $g_1 = -0.19$ recommended by Bender *et al.* [24] from their study of the Gamow-Teller resonances.

where $\beta = (3\pi^2/2)^{2/3}$, and $N_0^{-1} = \pi^2\hbar^2/2m^\star k_F$ is an effective-mass-dependent normalization factor. The Skyrme-force-induced g_0 and g_1 parameters (Fig. 1) are indeed scattered rather randomly, reflecting the fact that Skyrme forces are fitted ultimately to the TE channel while the TO components of the S-LEDF are only cross-checked mostly through high-spin (cranking) applications. In Ref. [24] the preferred values $g_0 = 0.4$, $g_0' = 1.2$, and $g_1 = -0.19$, $g_1' = 0.62$ have been established from an analysis of the Gamow-Teller resonances, see also Ref. [35] and references quoted therein. These values were obtained under the additional assumption that there is no density dependence for C_t^s and that $C_t^{\Delta s} \equiv 0$. The LEDF with spin fields defined in this way will be called the Landau-LEDF (L-LEDF).

A. The spin fields of the ground state

Before proceeding to the study of the terminating states, let us discuss the spin fields of the ground states (calculated

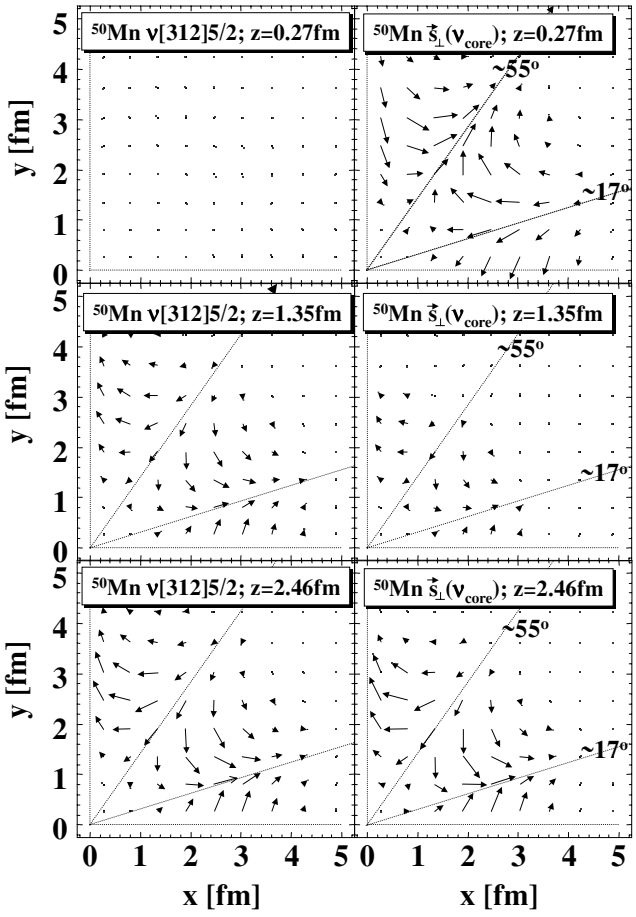

FIG. 2. The $\vec{s}_\perp$ component of the spin density (in arbitrary units) in the Oxy plane, calculated at three selected values of $z = 0.27$ fm (upper part), $z = 1.35$ fm (middle part), and $z = 2.46$ fm (lower part) of the ground state of ^{50}Mn. Left panels show the contribution of the odd neutron and right panels show the polarization effect exerted by the odd neutron on the neutron core. For this case $\vec{s}_\perp^{\,\nu} \approx \vec{s}_\perp^{\,\pi}$; see text for further detail.

in HF approximation) of $N \approx Z$ nuclei. It is known that the binding energies calculated using the complete S-LEDF functional exhibit a rather peculiar behavior in odd-odd $T_z = 0$ and some odd-A $|T_z| = 1/2$ nuclei [36]. It manifests itself via an additional binding energy of $\sim$1 MeV as compared to the SHF calculations using only the TE part of the S-LEDF. This effect disappears for $|T_z| > 1$ nuclei.

The enhancement in binding energy of $N \approx Z$ nuclei is due to a strong polarization effect exerted by the spin field of the odd particle(s) on the spin field of the core, as illustrated in Figs. 2 and 3 for a representative example of the manganese isotopes. Figure 2 shows the Oxy component of the spin density $\vec{s}_\perp$ in ^{50}Mn for three selected sections through this axially deformed nucleus, which include the near-equatorial plane at $z = 0.27$ fm as well as $z = 1.35$ and 2.46 fm planes. To visualize the polarization effect we decompose the spin density into contributions of the valence particles (note that $\vec{s}^{\,\pi} \approx \vec{s}^{\,\nu}$ in this $N = Z$ nucleus) and the core. The topology of the surfaces shown on the left-hand side reflects the structure of the dominant asymptotic [312]5/2 Nilsson component in the wave function of the valence particle. Indeed, the one particle contribution to the spin field in a simplex-conserving axial HO basis state

$$\Psi_{Nn_z|\Lambda|;s=\pm i} = \frac{1}{\sqrt{2}}(\Psi_{Nn_z\Lambda;1/2} \pm i\,\Psi_{Nn_z-\Lambda;-1/2}), \quad \text{where} \quad \Psi_{Nn_z\Lambda} = \psi_{Nn_z|\Lambda|}e^{i\Lambda\varphi}, \tag{9}$$

is

$$s_x = -\tfrac{1}{2}\left|\psi_{Nn_z|\Lambda|}(\rho,z)\right|^2 \sin 2\Lambda\varphi, \qquad s_y = -\tfrac{1}{2}|\psi_{Nn_z|\Lambda|}(\rho,z)|^2 \cos 2\Lambda\varphi, \quad s_z = 0, \tag{10}$$

see Ref. [12] for further details. Hence, $|s_x|/|s_y| = |\mathrm{ctg}2\Lambda\varphi|$ and the plot of $\vec{s}_\perp$ shows the characteristic *vortex* lines for $|s_x|/|s_y| = 1$, i.e., for $\varphi = [45^\circ + n\pi]/2\Lambda$, where $n = 0, 1, 2, \ldots$. Two such lines that appear in Fig. 2 are consistent with $\Lambda = 2$. Moreover, the small values of $s_{xy} \sim 0$ over the entire equatorial plane at $z = 0.27$ fm are due to $\psi_{[312]} \sim H_1(z \approx 0) \approx 0$. Our calculations also show that although $s_z \neq 0$, the condition $|s_z| \ll |s_\perp|$ is well fulfilled for most cases.

The correlation between the spin field $\vec{s}_\perp^{\,\pi[512]}(\boldsymbol{r})$ due to the occupation of the [512]5/2 orbital by the valence proton and that of the core $\vec{s}_\perp^{\,\mathrm{core}}(\boldsymbol{r})$ (polarization effect) is illustrated in Fig. 3. The figure shows the product $|\vec{s}_\perp^{\,\pi[512]}(\boldsymbol{r})| \cdot |\vec{s}_\perp^{\,\mathrm{core}}(\boldsymbol{r})|$ that reflects the magnitude of the spin fields versus the classical angle θ between these vectors corresponding to their relative orientation. The figure clearly illustrates that the core polarization is strongest in o-o $N = Z$ nuclei and is almost of ferromagnetic type. In odd-A $N - Z = \pm 1$ nuclei, the effect is reduced but still remains. Hence, the role of the spin fields in these nuclei is maximal. In $|N - Z| > 1$ nuclei, the induced (core) spin field becomes quenched and is not any more coherent with the valence-particle(s) spin field, particularly in o-o nuclei, as depicted in Fig. 3(c).

At least two very important conclusions can be drawn from this analysis. (i) The coherence of the spin fields in $N \sim Z$ nuclei may cause a strong polarization of the nucleus. (ii) The magnitude of the spin-field-induced effects is predicted to depend strongly on isospin. These two observations give us a unique opportunity to resolve the strength of the spin fields, in particular, by using high spin states where spin fields are expected to be enhanced.

B. The spin fields at the band termination

Figure 4(a) shows the calculated energy differences for the terminating states $\Delta E_{\mathrm{th}} = E_{\mathrm{th}}[d_{3/2}^{-1} f_{7/2}^{n+1}] - E_{\mathrm{th}}[f_{7/2}^{n}]$ relative to the experimental data ΔE_{exp} given in Table I, i.e., the values of $\Delta E \equiv \Delta E_{\mathrm{exp}} - \Delta E_{\mathrm{th}}$. The first striking observation stemming from this calculation is that *all* considered Skyrme forces systematically underestimate the empirical data by at least 10%. In the case of the SkM* and SkP parametrizations, the difference even exceeds 20–30%. The disagreement is unexpectedly large given the structural simplicity of the terminating states.

Let us further observe that the values of ΔE calculated using SLy4 and SLy5 forces, which are in general rather similar to ΔE obtained using SIII or SkO forces, increase rapidly

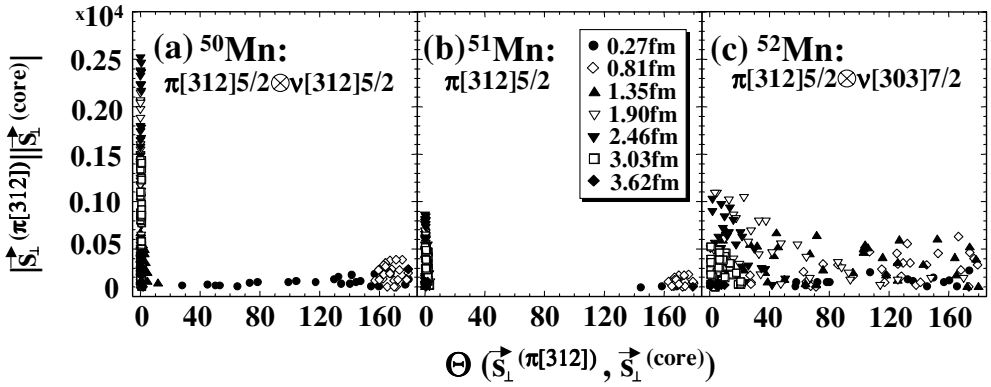

FIG. 3. Product of $|\vec{s}_\perp^{\,\pi[512]}(\boldsymbol{r})||\vec{s}_\perp^{\,core}(\boldsymbol{r})|$ reflecting the magnitude of the spin fields (in arbitrary units) versus the classical angle θ between these vectors, corresponding to their relative orientation. (a) $N = Z$ o-o nucleus ^{50}Mn, (b) $N - Z = 1$ odd-A nucleus ^{51}Mn, (c) $N - Z = 2$ o-o nucleus ^{52}Mn. All the points that are calculated at a fixed value of the z coordinate and different values of the (x,y) coordinates are labeled by the same symbol, as indicated in the legend.

in $N - Z = 1$ nuclei ^{47}V and ^{45}Ti. This result is related to the magnitude of the spin fields and the ferromagnetic-type polarization of the core which, as discussed in the preceding section and in Ref. [36], are exceptionally large for Lyon forces; see also Fig. 1. Since no enhancement of this type is observed in the data, this result clearly shows that a unified description of the spin fields within the LEDF theory is required.

Hence, we state that the experimental data suggest a generalization of the S-LEDF. However, our strategy is to introduce a minimal-type modification that ultimately pertains only to the TO part of the S-LEDF. More precisely, for SLy4, SIII, SkO, and SkM* we change the spin fields, i.e., the first two terms of the TO part of the LEDF (5) not affecting the local gauge invariance (6). For SkP, SkXc, and SLy5, on the other hand, we also slightly modify the TO part of the tensor term. In this way we actually brake the local gauge invariance. However, our calculations show that this has a very small effect on the final results when compared to calculations using the Skyrme-force-induced C_t^T values. Thus, one can state that the local gauge invariance (6) is in fact preserved in our calculations.

Our favorite unification scheme for the treatment of the spin fields (called L-LEDF) follows the one developed by Bender *et al.* [24]. Let us recall that in the L-LEDF calculations we assume density-independent coefficients C_t^s defined through the Landau parameters $g_0 = 0.4$, $g_0' = 1.2$, $g_1 = -0.19$, and $g_1' = 0.62$ and set $C_t^{\Delta s} = 0$. Such a simple treatment of the spin fields leads to a surprisingly consistent picture for the various Skyrme forces, irrespective of the difference in effective mass. Indeed, the results obtained for all forces, except those of SkM* and SkP, essentially overlie each other as shown in Fig. 4(b). We suspect that the effective mass or, equivalently, the current independence of our results is directly related to the gauge invariance of the LEDF. This point requires, however, further investigation. Let us further observe that ΔE calculated with SkM* and SkP show almost a constant offset as compared to the other forces.

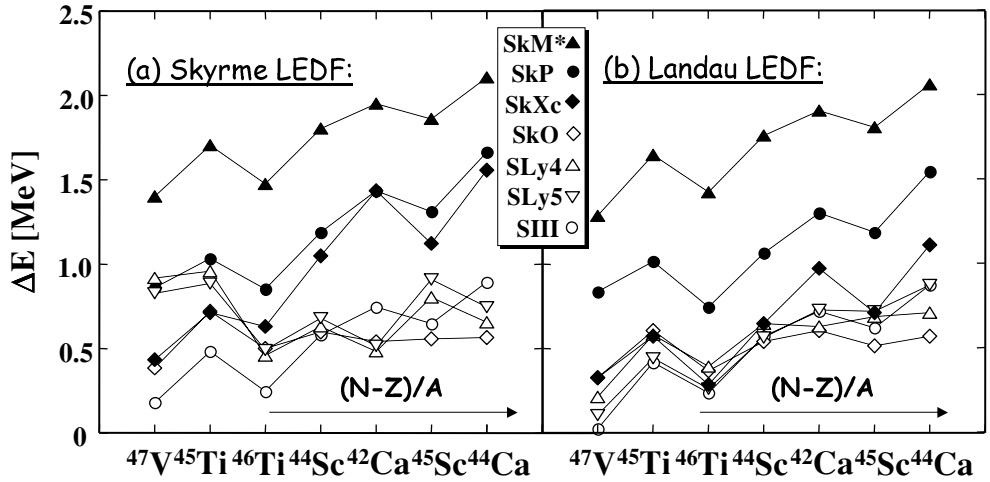

FIG. 4. Calculated energy differences for the terminating states $\Delta E_{\rm th} = E_{\rm th}[d_{3/2}^{-1} f_{7/2}^{n+1}] - E_{\rm th}[f_{7/2}^{n}]$ relative to the experimental data $\Delta E \equiv \Delta E_{\rm exp} - \Delta E_{\rm th}$, where $\Delta E_{\rm exp}$ are listed in Table I. (a) SHF calculations; (b) calculations using L-LEDF.

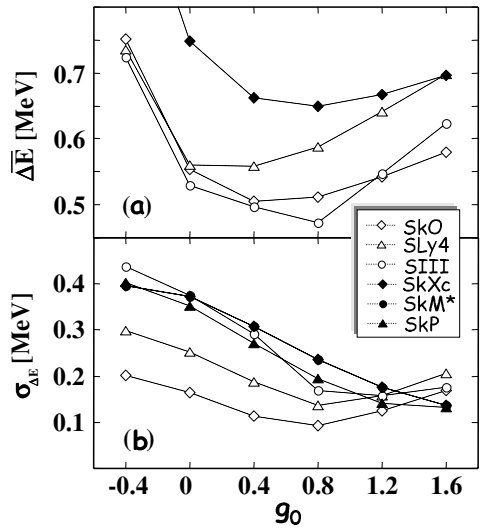

FIG. 5. (a) The average difference $\overline{\Delta E}$ ($\Delta E \equiv \Delta E_{\rm exp} - \Delta E_{\rm th}$) and (b) the standard deviation σ between the data and the calculations versus Landau parameter g_0.

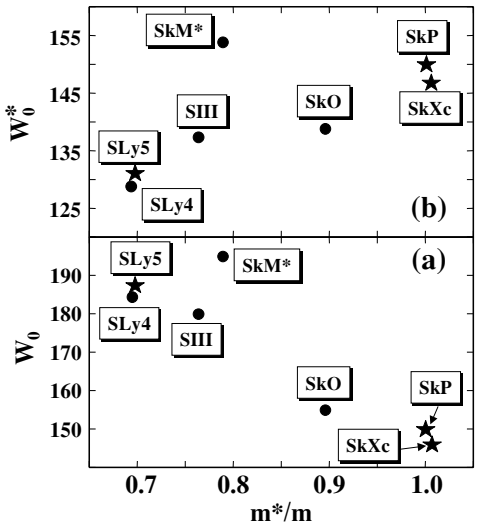

FIG. 6. (a) The strength W_0 and (b) the effective-mass-scaled strength $W_0^\star$ of the isoscalar part of the spin-orbit SHF potential versus the effective mass. Filled dots denote parametrizations that do not include tensor densities; stars denote those that do. See text for more detail.

Since we focus on $N \sim Z$ nuclei, our calculations cannot be used to determine the isovector Landau parameters g_0' and g_1'. However, the sensitivity of our predictions with respect to the isoscalar Landau parameter g_0 is striking, as seen in Fig. 5. Figure 5(a) shows the average deviation from the data $\overline{\Delta E}$ versus g_0. Note that $\overline{\Delta E}$ is minimal for $g_0 \sim 0.4$–0.8, which is very close to the suggested value $g_0 = 0.4$ of Ref. [24]. Let us further observe that $\overline{\Delta E}$ does not change sharply within the interval $\Delta g_0 = \pm 0.4$ around the preferred value, but our analysis seems to rule out both negative and large positive (>1.2) values of g_0. Moreover, the remaining ~10% discrepancy between the calculations and the data cannot be accounted for by further readjusting the Landau parameters, at least not within the analyzed unification scheme.

Figure 5(b) shows the dependence of the standard deviation $\sigma_{\Delta E}$, which reflects the spread in ΔE, on g_0. Apparently the minimum is obtained for $g_0 \sim 0.8$–1.2, i.e., well above the preferred value of $g_0 = 0.4$. Let us observe, however, that almost all curves in Fig. 4 clearly show an increasing trend as a function of the reduced isospin $T_A \equiv (N - Z)/A$. Hence, part of the spread may merely reflect the isovector properties of the LEDF, most likely, the isovector part of the ℓs-term. The relatively weak dependence of ΔE on T_A obtained for the SkO force seems to support this conclusion. Additional analysis strengthening this scenario is given in the next section.

V. THE SPIN-ORBIT TERM

Within the SHF theory, the ℓs potential takes the form

$$V_{LS}(q, \boldsymbol{r}) = -i \boldsymbol{W}_q(\boldsymbol{r}) \boldsymbol{\nabla} \times \boldsymbol{\sigma}, \tag{11}$$

where $q = n$, p and

$$\boldsymbol{W}_q(\boldsymbol{r}) = \tfrac{1}{2} W \boldsymbol{\nabla} \rho_0(\boldsymbol{r}) + \tfrac{1}{2} W' \boldsymbol{\nabla} \rho_q(\boldsymbol{r}) - \tfrac{1}{8}[(t_1 x_1 + t_2 x_2) \boldsymbol{J}(\boldsymbol{r}) + (t_2 - t_1) \boldsymbol{J}_q(\boldsymbol{r})]. \tag{12}$$

The vector spin density $\boldsymbol{J}(\boldsymbol{r})$ dependent terms contribute rather weakly to the ℓs potential. Hence, the magnitude of the ℓs potential is determined essentially by the first two terms in Eq. (12). For the spherical limit, the ℓs potential can be approximated by

$$V_{LS}(q, r) \approx \left\{ W \frac{1}{r} \rho_0'(r) + W' \frac{1}{r} \rho_q'(r) \right\} \boldsymbol{\ell s} = \left\{ \frac{W_0}{r} \rho_0'(r) \pm \frac{W_1}{r} \rho_1'(r) \right\} \boldsymbol{\ell s}, \tag{13}$$

where $\rho_0' = (\rho_n + \rho_p)'$ and $\rho_1' = (\rho_n - \rho_p)'$ are the radial derivatives of the local isoscalar and isovector densities, while $W_0 \equiv W + \frac{1}{2} W'$ and $W_1 \equiv \frac{1}{2} W'$ denote the isoscalar and isovector strengths, respectively. They are in turn related to the coupling constants of the S-LEDF of Eq. (4) through $C_t^{\nabla J} = -\frac{1}{2} W_t$.

A direct comparison of the isoscalar strengths W_0 of the ℓs-potential is given in Fig. 6(a). Apparently, SLy4, SLy5, SkM*, and SIII forces have a strong, while SkO, SkP, and SkXc have a weak ℓs potential assuming, of course, that there are no drastic differences in the isoscalar density profile. That assumption should be rather well fulfilled in light nuclei, which are considered here. It is interesting to note that the conclusions stemming from a direct comparison of W_0 are in complete contradiction to the results presented in Fig. 4. Indeed, according to our calculations, SLy4, SLy5, SkO, SIII, and eventually SkXc are expected to have similar ℓs strengths while those for SkM* and SkP should be considerably stronger.

The question therefore arises of how to compare the strengths of the ℓs potential for different parametrizations. The problem appears to be related to nonlocal effects which are, within the SHF, absorbed into the kinetic energy term through the effective mass m^*. The impact of nonlocalities on the ℓs potential can be studied using the so-called asymptotically

equivalent wave function [4,32]

$$\tilde{\phi}_i(\boldsymbol{r}) = \sqrt{\frac{m}{m^\star(\boldsymbol{r})}}\phi_i(\boldsymbol{r}). \tag{14}$$

This representation allows us to rewrite the SHF equations in an alternative form with a bare mass m in the kinetic energy term, a state-dependent central potential $U_q(e_\mu; \boldsymbol{r})$, and an effective-mass-scaled ℓs potential (13):

$$V_{LS}(q, r) \approx \frac{m^\star(r)}{m}\left\{\frac{W_0}{r}\rho_0'(r) \pm \frac{W_1}{r}\rho_1'(r)\right\}\boldsymbol{\ell s}. \tag{15}$$

The effective-mass-scaled isoscalar strengths $W_0^* \equiv \frac{m^\star}{m}W_0$ are depicted in Fig. 6(b). Note that the classification of the ℓs-strength according to W_0^* agrees very nicely with our results shown in Fig. 4. Indeed, the values of W_0^* are similar for SLy4, SLy5, SIII, and SkO and considerably larger for SkP and SkM*. This indicates that at least part of the observed discrepancy $\overline{\Delta E}$ results from a too strong ℓs term. By reducing the strength by ∼5%, $\overline{\Delta E}$ decreases by ∼350 keV bringing it to an acceptable level of ∼200 keV for most of the forces. In particular, for the case of the SkO force, $\overline{\Delta E}$ drops from 504 to 164 keV, while for SLy4 a 5% reduction of the ℓs strength decreases $\overline{\Delta E}$ from 560 to 189 keV. Our analysis indicates that a reasonable strength lies in the range of $W_0^* \approx 123$–133.

Concerning the isovector ℓs potential, the Skyrme forces discussed in the literature can be divided into three major classes. The standard Skyrme force parametrizations assume that $W = W'(W_1/W_0 = 1/3)$, implying that $\boldsymbol{W}_q \sim W(2\rho_q' + \rho_{-q}')$. The SLy4, SLy5, SkM*, and SIII are standard forces among those studied here.

Nonstandard Skyrme interactions with $W \neq W'$ were first studied by Reinhard and Flocard [37] in connection with isotope shifts in Pb nuclei. Consistency with experimental data led them to the parametrizations with $W' \sim -W$ or $(W_1/W_0 = -1)$, i.e., to an entirely different isovector dependence of the ℓs-term $\boldsymbol{W}_q \sim W\rho_{-q}'$. The study of the ℓs term in neutron-rich nuclei by Reinhardt *et al.* [33] seems further to corroborate this result. The so-called SkO parametrization established in Ref. [33] (and studied here) has an even larger negative value of W_1 with $W_1/W_0 \approx -1.3$.

The third type of ℓs term considered in the literature in connection with the SHF approach was introduced by Brown [30], who uses $W' = 0$ (parametrization SkXc). In this case, there is no isovector ℓs term $(W_1/W_0 \equiv 0)$ and $\boldsymbol{W}_q \sim W(\rho_n' + \rho_p')$.

As already discussed at the end of Sec. IV B our calculations give certain preference to the SkO-induced L-LEDF, since it minimizes the spread in ΔE, $\sigma_{\Delta E}$. In particular, our results seem to favor a ℓs potential with large negative isovector strength W_1. To corroborate this observation we performed a set of calculations based on the SkO-induced L-LEDF; at the same time, we explored different isovector dependences of the ℓs term, including the four possibilities discussed above, namely $W_1/W_0 = -1.3, -1, 0$, and 1/3. In the calculations, the isoscalar strength W_0 was kept constant and its value was reduced by 5% as compared to the original SkO strength.

The calculated values of ΔE for these four variations of the SkO-induced L-LEDF are shown in Fig. 7. A change in the

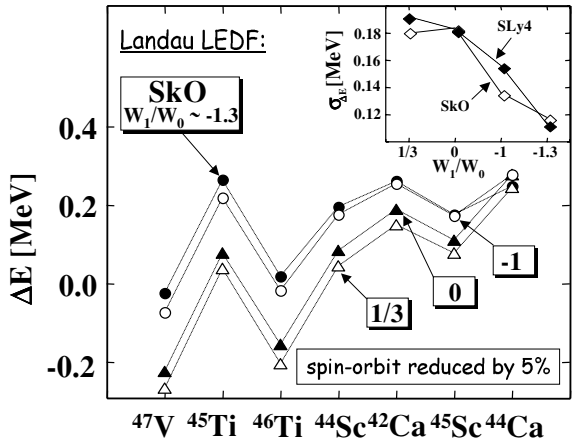

FIG. 7. The values of ΔE calculated using the SkO-induced L-LEDF with four different parametrizations of the isovector ℓs-term, including the original $W_1/W_0 \approx -1.3$ strength and the modified strengths $W_1/W_0 = -1$, 0, and 1/3. In the calculations, W_0 was fixed at 5% below its original value. The insert shows the dependence of the spread in ΔE, $\sigma_{\Delta E}$, on W_1/W_0 calculated for the SkO-induced and the SLy4-induced L-LEDF.

W_1/W_0 ratio from the (near) original values -1.3, -1 to 0, 1/3 clearly destroy the agreement to the data. Indeed, the spread $\sigma_{\Delta E}$ increases from 113 and 136 keV $(W_1/W_0 = -1.3, -1)$ to 184 and 180 keV $(W_1/W_0 = 1/3,\ 0)$, respectively; see insert in Fig. 7. Note, however, that since we deal with $N \sim Z$, a fine tuning of the isovector terms cannot be achieved.

Similar calculations with the SLy4-induced L-LEDF, corroborate our conclusions. The change of the W_1/W_0 ratio from the (near) original values 1/3, 0 to –1,–1.3 improves the agreement to the data, as shown in the insert in Fig. 7. Note also, that the calculated spread $\sigma_{\Delta E}$ is quantitatively very similar for both the SkO-induced and SLy4-induced L-LEDF provided the isovector part of the ℓs term is similar.

VI. SUMMARY

We have performed a systematic study of terminating states in the $A \sim 50$ mass region using the self-consistent Skyrme-Hartree-Fock model and testing several parametrizations of the Skyrme force. The objective was to demonstrate that the terminating states, because of their intrinsic simplicity, offer a unique and so far unexplored opportunity to study different aspects of the effective *NN* interaction or nuclear local energy density functional within the self-consistent approaches.

We have shown that the Skyrme-force parametrizations used in our work, including SLy4, SLy5, SkO, SIII, SkXc, SkP, and SkM*, have a rather mediocre performance (for SkP and SkM* it is even unacceptable) for a seemingly simple observable like the energy difference between the aligned $f_{7/2}^n$ and $d_{3/2}^{-1}f_{7/2}^{n+1}$ states.

We further demonstrated that a simple unification of the spin fields according to the scheme proposed in Ref. [24] leads to a unified description of the data for SLy4, SLy5, SkO, SIII, and SkXc, i.e., for very different parametrizations. This

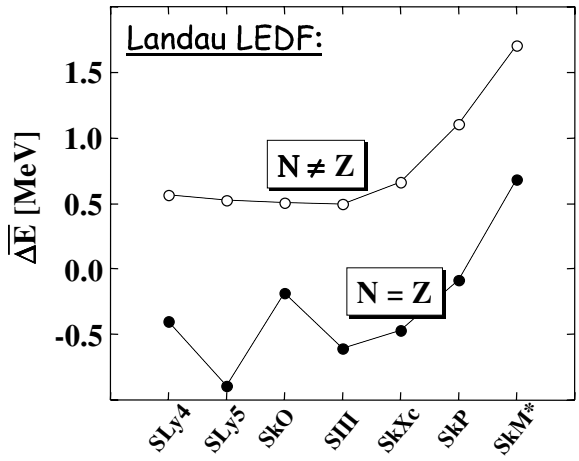

FIG. 8. The average deviation $\overline{\Delta E}$ for $N \neq Z$ (open dots) and for $N = Z$ (filled dots) nuclei. The latter case includes data for ^{44}Ti [19] where $E[f_{7/2}^n]_{12^+} = 8.038$ MeV, $E[d_{3/2}^{-1} f_{7/2}^{n+1}]_{15^-} = 13.369$ MeV, and $\Delta E_{\text{exp}} = 5.331$ MeV, and for ^{46}V [38] where $E[f_{7/2}^n]_{15^+} = 8.484$ MeV, $E[d_{3/2}^{-1} f_{7/2}^{n+1}]_{17^-} = 13.629$ MeV, and $\Delta E_{\text{exp}} = 5.145$ MeV. All calculations were done using the L-LEDF.

result seems to indicate the importance of the local gauge (and Galilean) invariance of the local energy density functional. The remaining discrepancy of ∼500 keV (see Fig. 8), which is still ∼10%, cannot be reduced by further readjusting the spin fields.

The remaining disagreement between theory and experiment for different parametrizations correlates nicely with the values of the effective-mass-scaled isoscalar strength of the ℓs term for these parametrizations. Hence, a part of this discrepancy can, most likely, be ascribed to a too strong isoscalar ℓs term. A reduction of the isoscalar ℓs strength by 5% reduces the discrepancy well below the 5% level. Moreover, our calculations suggest that the spread in ΔE can be further reduced by adopting the nonstandard parametrizations of the ℓs term with a strong negative isovector strength $W_1/W_0 \leqslant -1$.

Finally, let us point out that there is a large difference in $\overline{\Delta E}$ calculated in $N \neq Z$ and $N = Z$ nuclei; see Fig. 8. For $N \neq Z$ our L-LEDF approach systematically underestimates the data, while the opposite is true for $N = Z$ nuclei. The offset between the two curves is ∼1 MeV. This result leaves us with an extremely important question: Does this offset indicate the breakdown of the standard mean field in $N \sim Z$ nuclei and the need for substantial configuration mixing even for the terminating states [39] and what is the possible source of such mixing?

ACKNOWLEDGMENTS

The authors thank Sylvia Lenzi and Jan Styczeń for communicating experimental results prior to publication. One of us (W.S.) is grateful to J. Dobaczewski for stimulating discussions and many constructive comments on the manuscript. This work was supported by the Foundation for Polish Science (FNP), the Göran Gustafsson Foundation, the Swedish Science Council (VR), the Swedish Institute (SI), and the Polish Committee for Scientific Research (KBN) under Contract No. 1 P03B 059 27.

[1] A. V. Afanasjev, D. B. Fossan, G. J. Lane, and I. Ragnarsson, Phys. Rep. **322**, 1 (1999).
[2] W. Satuła and R. Wyss, Rep. Prog. Phys. **68**, 131 (2005).
[3] K. Rutz, M. Bender, P.-G. Reinhard, J. A. Maruhn, and W. Greiner, Nucl. Phys. **A634**, 67 (1998).
[4] M. Lopez-Quelle, N. Van Giai, S. Marcos, and L. N. Savushkin, Phys. Rev. C **61**, 064321 (2000).
[5] I. Hamamoto and P. Siemens, Nucl. Phys. **A269**, 199 (1976).
[6] V. Bernard and N. van Giai, Nucl. Phys. **A348**, 75 (1980).
[7] A. Oros, Ph.D. thesis, University of Köln, 1996.
[8] A. Swift and L. R. B. Elton, Phys. Rev. Lett. **17**, 484 (1966).
[9] H. Tyren, S. Kullander, O. Sundberg, R. Ramachandran, P. Isacsson, and T. Berggren, Nucl. Phys. **79**, 321 (1966).
[10] L. Ray and P. E. Hodgson, Phys. Rev. C **20**, 2403 (1979).
[11] V. I. Isakov, K. I. Erokhina, H. Mach, M. Sanchez-Vega, and B. Fogelberg, Eur. Phys. J. A **14**, 29 (2002).
[12] J. Dobaczewski and J. Dudek, Comput. Phys. Commun. **131**, 164 (2000).
[13] J. Dobaczewski, J. Dudek, and P. Olbratowski, Comput. Phys. Commun. **158**, 158 (2004); HFODD User's Guide, nucl-th/0501008.
[14] S. G. Nilsson, Dan. Mat.-Fys. Medd. **29**, 1 (1955).
[15] A. Bohr, I. Hamamoto, and B. Mottelson, Phys. Scr. **26**, 267 (1982).
[16] C. Bahri, J. P. Draayer, and S. A. Moszkowski, Phys. Rev. Lett. **68**, 2133 (1992).
[17] J. Ginocchio, Phys. Rev. Lett. **78**, 436 (1997).
[18] M. Lach *et al*., Eur. Phys. J. A **16**, 309 (2003).
[19] S. Lenzi and J. Styczeń (private communication).
[20] M. Lach *et al*., Eur. Phys. J. (to be published).
[21] P. Bednarczyk *et al*., Acta Phys. Pol. B **32**, 747 (2001).
[22] F. Brandolini *et al*., Nucl. Phys. **A693**, 517 (2001).
[23] J. Dobaczewski and J. Dudek, Phys. Rev. C **52**, 1827 (1995); C **55**, E3177 (1997).
[24] M. Bender, J. Dobaczewski, J. Engel, and W. Nazarewicz, Phys. Rev. C **65**, 054322 (2002).
[25] Y. M. Engel, D. M. Brink, K. Goeke, S. J. Krieger, and D. Vautherin, Nucl. Phys. **A249**, 215 (1975).
[26] P. Hohenberg and W. Kohn, Phys. Rev. B **136**, 864 (1964).
[27] W. Kohn and L. J. Sham, Phys. Rev. A **140**, 1133 (1965).
[28] W. Kohn, Rev. Mod. Phys. **71**, 1253 (1998).
[29] J. Dobaczewski, H. Flocard, and J. Treiner, Nucl. Phys. **A422**, 103 (1984).
[30] B. A. Brown, Phys. Rev. C **58**, 220 (1998).
[31] E. Chabanat, P. Bonche, P. Haensel, J. Meyer, and R. Schaeffer, Nucl. Phys. **A627**, 710 (1997); **A635**, 231 (1998).

[32] M. Beiner, H. Flocard, N. Van Giai, and P. Quentin, Nucl. Phys. **A238**, 29 (1975).
[33] P.-G. Reinhard, D. J. Dean, W. Nazarewicz, J. Dobaczewski, J. A. Maruhn, and M. R. Strayer, Phys. Rev. C **60**, 014316 (1999).
[34] J. Bartel, P. Quentin, M. Brack, C. Guet, and H. B. Håkansson, Nucl. Phys. **A386**, 79 (1982).
[35] F. Osterfeld, Rev. Mod. Phys. **64**, 491 (1992).
[36] W. Satuła, in *Nuclear Structure 98*, edited by C. Baktash, AIP Conf. Proc. No. 481 (AIP, Woodbury, NY, 1999), p. 114; nucl-th/9809089.
[37] P.-G. Reinhard and H. Flocard, Nucl. Phys. **A584**, 467 (1995).
[38] S. Lenzi *et al*., Phys. Rev. C **60**, 021303 (1999).
[39] J. Terasaki, R. Wyss, and P.-H. Heenen, Phys. Lett. **B437**, 1 (1998).